ISSN 2706-655X Vol.5, Issue 10: 77-86, DOI: 10.25236/IJFET.2023.051012

A Wire-driven Full Constraint Mechanical Long Arm with Digital Control

Shengcong Wang

The Stony Brook School, New York, USA
zhenglei@co-effort.com

Abstract: *Manipulators have been widely used in modern industrial fields. The long arm with wire control has the advantages of light arm body structure, separation of control part with the execution arm, and long length with more flexibility in control, which makes it able to serve a wider range of application scenarios, especially many highly-radiation, polluted and confined environments, and greatly reduce the risks of injury to people and property during operation. In order to make a safe and easily operated mechanical arm which can be used for polluted environments, the author of this paper tried to use his knowledge and research experience to design and make a low-cost and environmentally friendly ultra-redundant wire-controlled long arm with the safe and easily available materials and components. The author designed and implemented a mechanical long arm with a universal joint structure driven by steering gears and a wire-controlled transmission. The arm body is composed of 8 controlled universal joints connected in series. It is controlled in two groups, and each group can realize two degrees of freedom, the 4 joints in a group ensure the same rotation angle through the mechanical structure. At the same time, the mapping model of motor and cable, and the mapping model of cable and rotation angle are constructed to realize the movement of the control unit at a given angle, and the author's design is verified by experiments.*

Keywords: *manipulator, mechanical arm, long arm, wire-driven*

1. Introduction

With the improvement of the degree of automation of industrial production, the wide application of robots in industry, research works, or even our daily life is an irreversible trend. In many cases, robots and mechanical arms can replace humans for dangerous, dirty work, increase productivity levels, address labor shortages and reduce the likelihood of human error due to fatigue. However, injury accidents occurred from time to time.

First, compared with traditional mechanical arms, the wire-controlled mechanical arms are light in weight and highly flexible in control. Light weight and high flexibility greatly reduce their risk of injury to people and property and make them safer. Second, compared with a traditional mechanical arm, the arm of a wire-controlled mechanical arm is structurally separated from its body, and its arm responsible for execution does not contain any circuit components. The control part, which can be easily affected by high pressure, radiation or pollution environments, is placed in a remote position, which can avoid the source of the impact and also be easily repaired in case of any breakdown. Therefore, the wire-driven manipulators can be used for complex work in confined, narrow or polluted areas.

Through research of the works related to hyper-redundant manipulators and utilizing my knowledge of space transformation matrix learned in linear algebra class, I decided to design and make a wire-driven mechanical arms with the low-cost, light and safe materials and components. By making it, I had a deeper understanding of the feature of a wire-driven full constraint mechanical long arm with digital control and identified the potential problems and obstacles in making the real wire-controlled long arm for industrial use as well[1-2].

In this paper, I described the process of designing and making a wire-driven mechanical long arm with digital control. Not only did I successfully design and make the manipulator with the low-cost and safe materials and components easily available to a student, but also, after several iterations, I used two experiments to evaluate the operations of the finished manipulator. The rest of the paper is organized as follows: Section 2 describes my structural and mechanical design with the detailed information about the control module and structure; Section 3 depicts two sets of experiments to test the manipulator; Section 4 concludes the paper by summarizing the functions realized and future research directions.

2. Method

2.1 Engineering Objectives

Since the 1960s, a lot of research has been done on hyper-redundant manipulators. Today, hyper-redundant manipulators can be classified into the following three categories, ie. Module joints manipulator, Cable-driven long arm manipulator and Continuum joints manipulator. Among them, some research is focused on the control algorithm, while some focus on the materials and structure. When designing my own manipulator, I decided to make a cable-driven long arm because it has the advantages of light weight and allowing longer length, which can make the manipulator safer and more environmentally friendly.

In order to achieve a lighter weight, I chose wooden boards. which could be made to the shapes I need using laser cutting. I also used some parts made by a 3D printer. For the transmission cable, I identified kit string for its light weight, strength, toughness, rigidity and convenient availability.

In order to achieve greater flexibility, I designed and built a four degrees of freedom mechanical long arm with eight sections and two groups of control. Such design not only realized the high flexibility but also allowed to add the length of the arm very easily[3-6].

Combined with my knowledge in mathematics, physics, and programming, I created a control module, which can control the manipulator's actions according to the input pitch angle and azimuth angle.

My manipulator consists of a base and a long arm, which is a multi-joint structure with 8 controlled universal joints connecting the sections. Since my motor could only provide limited torque, I set four servos for each joint to control the pitch rotation and left/right rotation of the universal joint, with two servos working together to drive one degree of freedom. The motors are mounted on the base to reduce the weight of the arm. They are connected to the universal joint through cables to provide transmission. This design achieved the mapping between the motor rotation and cable length, as well as between the cable and joint rotation angle. Through the calculation of the controller, the joint can be rotated according to the given angle. The eight universal joints are divided into two groups for control. Four universal joints are controlled by the same control unit to ensure the same rotation angle of each joint through a pre-tensioning mechanism. As is shown in Fig 1.

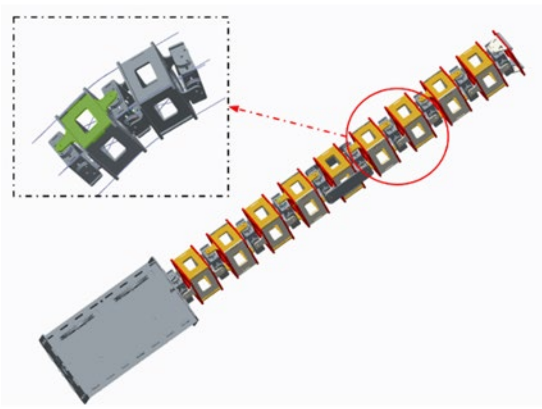

Figure 1: Version III 3D model

2.2 Structural Design

My initial design was a relatively simple manipulator, consisting of a circular base and six sections of manipulator arm. A universal joint would be used to join the two sections. The servo motors installed on the base drives the rotation of the universal joints through cables. Each universal joint would be driven by two servo motors, each of which drives the universal joint with one degree of freedom. However, I found two problems.

1)The total length of the manipulator is less than half a meter, which is not very practical. If the arm body needs to be longer, the motor is prone to overload. In addition, the longer the section of manipulator body, the larger the steering radius in the pipeline, making the manipulator unable to operate in some narrow pipelines.

ISSN 2706-655X Vol.5, Issue 10: 77-86, DOI: 10.25236/IJFET.2023.051012

2)The control of four manipulator sections requires too much computing power of the CPU on the motherboard. Therefore, it is not scalable if more sections are to be added.

For the first problem, I decided to change the original four sections of fully constrained control to eight sections of unconstrained control. This could be done by using only two control units consisting of four sections each. This design not only solved the problem of limited length, but also improved the scalability of the electric control[7-11].

Figure 2: Overview of the finished Manipulator

1) Manipulator Body

As is shown in Fig 2, there are altogether 10 universal joints. But the first joint counting from the base has only 1 degree of freedom. To compensate for the missing 1 degree of freedom, I fixed the 5th and 6th joint with 2 plates. In this way, the 5th joint has only 1 degree of freedom, too. The first control unit, comprising of joint 1 to joint 5, has 2 degrees of freedom. The same situation happens to the second control unit, comprising of joint 6 to joint 10. So the manipulator body has 8 controlled universal joints. This design is scalable. Further control units can be easily added.

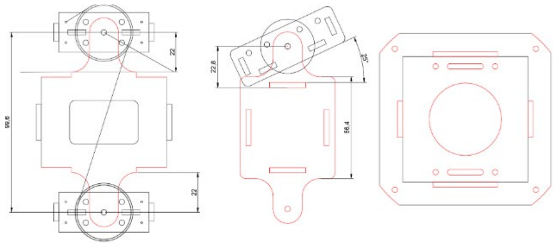

Figure 3: The Third Generation Manipulator Body Drawing

As is shown in Fig 3, the design of manipulator body was changed to a rectangle. This adjustment not only enhanced the stability, but also allowed for convenient assembling of the wire tube. Moreover, as shown above, the main drive of the manipulator can go through the four corners of the arm instead of the middle of the arm. This saves space in the arm and increases the stability of the drive cable.

2) Base

The Fig 4 shows the design of the third generation of the chassis. The overall design has changed a lot because the original stepper motor drive was changed to a servo drive.

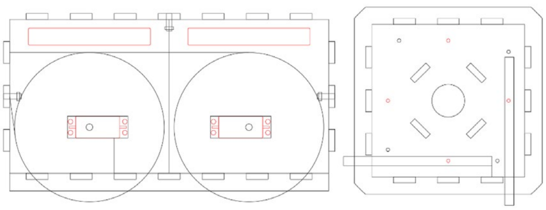

Figure 4: The Base Drawing

ISSN 2706-655X Vol.5, Issue 10: 77-86, DOI: 10.25236/IJFET.2023.051012

The new base has two servos fixed on each of the four internal surfaces. Each servo is connected to a round wheel. The role of the round wheel is mainly to fix the drive line and precisely control the distance to be pulled. Each degree of freedom is driven by two servos to ensure sufficient power[12-15].

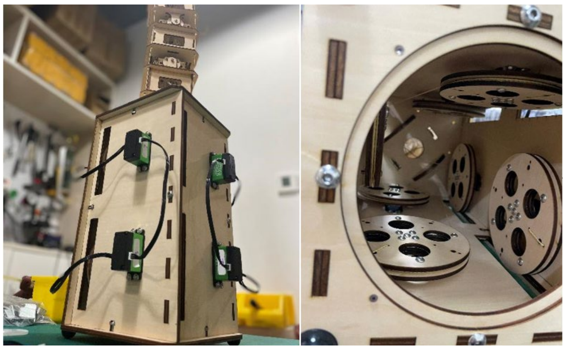

Figure 5: Outside and Inside of the Base

As is shown in Fig.5, the driving wheel is made up of three pieces of wood boards clamped together. The drive cable is fixed on one of the chords of the driving wheel. As the steering gear drives the wheel to rotate, the drive cable will be pulled. The stroke can be calculated by the circumference of the drive wheel.

3) Driving Cable and Pre-tensioning Mechanism

As shown in the figure, in the new version of the manipulator, I moved the position of the wire control drive from inside the manipulator to the four corners of each section of the manipulator, in order to provide as large arm of force as possible to compensate the lack of torque provided by the motors.

As Figure 6 shows, the wires connect the 1st control unit at the fifth segment. To ensure the segments of the control group bends in a controlled manner, I introduced the pre-tensioning mechanism.

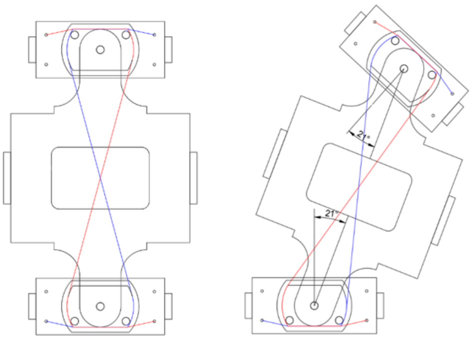

Figure 6: Pre-tensioning Mechanism

As shown in figure 6, when the manipulator body rotates 21° relative to the lower universal joint, the red line is pulled down and drives the upper universal joint to also rotate 21°. And when the manipulator body turns in the opposite direction, the blue line will function the same. This structure can ensure that the rotation angle of the second universal joint is exactly the same as that of the first universal joint. In my manipulator, the first to second and third to fourth universal joints of each control unit have this pre-tensioning structure. There is a same structure between the first and third universal joints on the other side. This pre-tensioning mechanism ensures that the rotation of any joint can be transmitted to other joints in the same control unit at the same angle.

2.3 Electronic Design

As shown in the figure 7, I used the ESP32 control board as the control motherboard for the 3rd generation manipulator. The servo driver board will transform the rotation angles got from the mother board to electrical signal and send to the relevant motor.

ISSN 2706-655X Vol.5, Issue 10: 77-86, DOI: 10.25236/IJFET.2023.051012

Figure 7: ESP32 Servo & Driver Board

4) Movement/Software Control/Programming

After the manipulator starts running, the CPU will parse the command got from the computer and get four angle values (two angles for each of the two control units). After the four values went through the matrix calculation, the CPU will send detailed servo motion instructions to the drive module. The logic is shown in Fig.8.

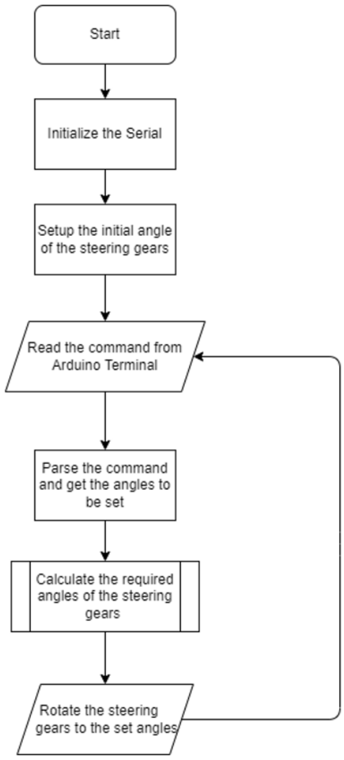

Figure 8: Logic Diagram of the Program

5) Mathematical Model

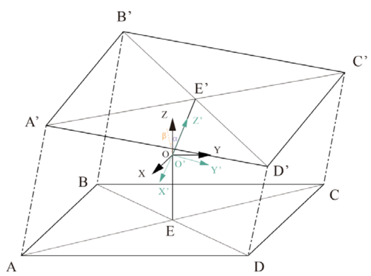

Figure 9: Interconnected Universal Joint Analysis

As shown in the figure 9, ABCD represents the top square of one segment and A 'B 'C 'D 'represents the bottom square of the next segment. As you can see, we set up two coordinate systems, xyz coordinate system corresponds to ABCD and x 'y 'z coordinate system corresponds to A 'B 'C 'D ', and x 'y 'z coordinate system is the rotation of xyz coordinate system. The coordinates of A 'B 'C 'D ' are easily represented in the x 'y 'z coordinate system. They just have same X and Y coordinates in its corresponding x 'y 'z' coordinate system as those of ABCD in xyz coordinate system. We need to get the coordinates of

ISSN 2706-655X Vol.5, Issue 10: 77-86, DOI: 10.25236/IJFET.2023.051012

A 'B 'C 'D ' in xyz coordinate system. And it can be done by multiplying a rotation matrix.

x-axis rotation matrix:

$$\begin{pmatrix} 1 & 0 & 0 \\ 0 & \cos\beta & \sin\beta \\ 0 & -\sin\beta & \cos\beta \end{pmatrix} \tag{1}$$

y-axis rotation matrix:

$$\begin{pmatrix} cos\,\alpha & 0 & -sin\,\alpha \\ 0 & 1 & 0 \\ sin\,\alpha & 0 & cos\,\alpha \end{pmatrix} \tag{2}$$

Then we can get the coordinates of A 'B 'C 'D ' in xyz coordinate system by the following formula:

$$[A']_{xyz} = \begin{bmatrix} \cos\alpha & 0 & -\sin\alpha \\ 0 & 1 & 0 \\ \sin\alpha & 0 & \cos\alpha \end{bmatrix} \begin{bmatrix} 1 & 0 & 0 \\ 0 & \cos(\beta) & \sin(\beta) \\ 0 & -\sin(\beta) & \cos(\beta) \end{bmatrix} [A']_{x'y'z'} \tag{3}$$

Then I can use the distance formula (see (4)) to get the length of AA', BB', CC', and DD', named L1, L2, L3, L4, respectively.

$$|AB| = \sqrt{(x_A - x_B)^2 + (y_A - y_B)^2 + (z_A - z_B)^2} \tag{4}$$

To obtain the distance change of the four wires, I need to subtract 44mm (initial length of each wire) from the four distances L1, L2, L3, L4. Then multiply the differences by 4 to find the total distance change of the entire control unit.

$$L^T = (L - 44) \times 4 \tag{5}$$

The radius of the drive wheel is 40mm, which means that the angle of rotation of the drive wheel corresponds to the actual stroke can be converted using the following equation.

$$L^T = \frac{\theta°}{360°} \times 2\pi \times 40 \tag{6}$$

Merging equation (5) and (6), I can find the rotation angle for the servo:

$$\frac{\theta}{360°} \times 2\pi \times 40 = (L - 44) \times 4 \tag{7}$$

$$\theta° = \frac{(L-44)\times 4\times 180°}{\pi\times 40} \tag{8}$$

Meanwhile, what I send to the servo is a number from 0 to 1000, and it needs to take corresponding to the number I plan to make servo rotate 230 °. As a result, each issued instructions O are made to the rotation angle ϴ * 100/23. And after calculation I get

$$O = \frac{(L-44)\times 4\times 180\times 100}{\pi\times 40\times 23} \tag{9}$$

In this way, I can translate the angle I want to rotate into the instructions sent to the driving motor.

3. Results and Discussion

After the manipulator was finished, I ran two experiments to evaluate its operation.

3.1 Joint Angle Experiment

The first experiment is to investigate the error between the calculated angle of a single joint and the actual rotation. As is shown in Fig.10, the experiment was done in the following steps[16-17].

1)Fix the manipulator upside down on the support, set the background plate, install the camera and adjust its shooting angle.

2)Connect with the computer and initialize the angle of each joint to be vertical.

3)Swing the distal control unit around the y-axe, and set the swing parameters as 5°, 10°, 15° and 20° successively, and record the swing process through the camera;

4)Restore the initial state and change it to swing the proximal control unit at 5°, 10° and 15°

ISSN 2706-655X Vol.5, Issue 10: 77-86, DOI: 10.25236/IJFET.2023.051012

respectively, and record the swing process through the camera;

5)Use the software Tracker to import videos of the processes, and measure the swing angles of each joint.

Figure 10: Scene of Joint Angle Experiment

Table 1: Swing Data of Independent Unit

Only distal	Joint 1 (°)	Joint 2 (°)	Joint 3 (°)	Joint 4 (°)
5°	-2.5	3.2	-0.8	4.4
10°	10.5	9.5	5	8.3
15°	4.6	14.5	10.2	12.5
20°	15.4	18.6	20.6	15.8
Only proximal	Joint 1 (°)	Joint 2 (°)	Joint 3 (°)	Joint 4 (°)
5°	10.8	8.8	1.6	1.7
10°	5.2	6.4	14.1	10.8
15°	11.9	13.2	17.8	11.5
20°	14.6	20.3	18.9	16.8

The overall experimental results show that the actual rotation angle of the manipulator joint and the theoretical value are quite different. After analyzing the data, I found three main causes.

Table 2: Comparison Table of Drive Wire Stroke

	1st wire actual length (mm)	1st wire theoretical length (mm)	2nd wire actual length (mm)	2nd wire theoretical length (mm)	3rd wire actual length (mm)	3rd wire theoretical length (mm)	4th wire actual length (mm)	4th wire theoretical length (mm)
Distal 5°	5.96	27.52	0.12	0.33	5.72	26.85	0.12	0.33
Distal 20°	97.50	110.43	3.78	4.70	90.34	101.77	3.78	4.70
Proximal5°	31.68	27.52	0.64	0.33	30.38	26.85	0.64	0.33
Proximal20°	97.78	110.43	3.80	4.70	90.58	101.77	3.80	4.70

ISSN 2706-655X Vol.5, Issue 10: 77-86, DOI: 10.25236/IJFET.2023.051012

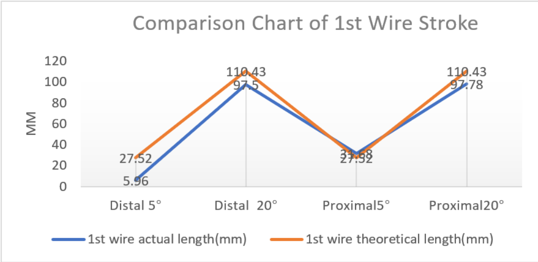

Figure 11: Comparison Chart of 1st Wire Stroke

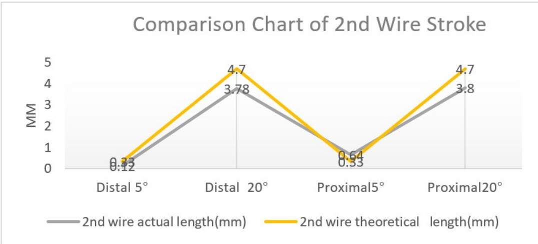

Figure 12: Comparison Chart of 2nd Wire Stroke

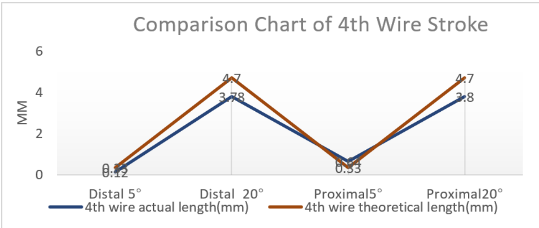

Figure 13: Comparison Chart of 3rd Wire Stroke

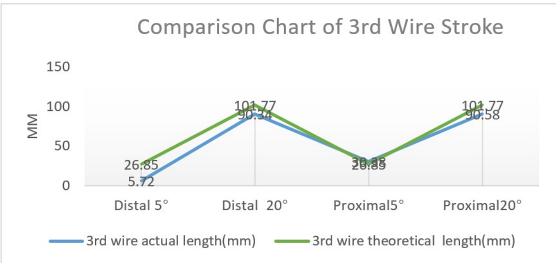

Figure 14: Comparison Chart of 4th Wire Stroke

1)As shown in the Table 1, Table 2 and Fig 11, 12, 13, 14, in most cases the actual angle is smaller than the theoretical angle, which means that the driving wire's change is less than the preset values. This is because the arm weight causes the string to be stretched, reducing the actual length pulled. This problem could be solved by replacing the kite string I currently use with steel wire, which is more rigid, or by changing the material of the manipulator arm from wood board to lighter carbon fiber.

2)I found that the rotation angle of each joint within a single control unit of the manipulator was inconsistent. However, according to the principle of pre-tensioning mechanism, the rotation angle of each joint should be consistent. After calculating the wire stroke, I find that the actual stroke is consistent with the preset value. The reason is that I wound the pre-tensioning mechanism manually, causing the different winding tightness. This inconsistency leads to the different torque required for rotating each joint. To solve this problem, I need to use more accurate tools to wind the wire and reduce the transmission wire clearance.

3)When the distal control unit rotates at a small angle, the actual rotation angle is negative. After analysis, this problem is found to be caused by the inaccurate initial value. As can be seen from the figure 4.1, section 4 has a bend in the absence of a swing angle, which is obviously caused by the initial value not being properly adjusted. However, due to the limited time and the inconsistent of clearance and winding tightness of the manipulator itself, I failed to find an optimal initial value.

3.2 Rectangular Motion Experiment

This experiment is to test the accuracy of rectangle movement with independent swing and matching swing of manipulator. As is shown in Fig.15, the experiment was done in the following steps.

1)Fix the manipulator upside down on the support, and fix the ping-pong ball at the end of the manipulator for video capture.

2)Enter the rectangular swing program to control the head of the manipulator to swing in accordance with the rectangle.

3)Put the mobile phone on the floor and shoot the moving track of the ping-pong ball at the end of the manipulator.

4)Install ruler for reference in video analysis process.

5)Set the swing parameters as (10,5) and (10,0), observe the changes, and record the video of the swing process.

6)Use Tracker to import videos and analyze the swing trajectory.

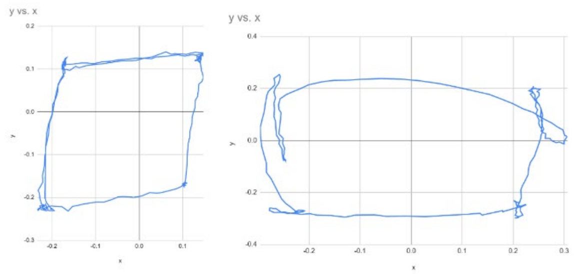

Figure 15: Spatial Position Capture

The experimental results are satisfactory: the difference between the motion trajectory and the theoretical trajectory is very small when only the distal units oscillate. However, the error of dual control unit is larger. After observation, I found that the main reason is that when the two control units move at the same time, the manipulator body appears to be shaking. There are two possible reasons for this shaking. First, the drive wire of kite string may be not rigid enough to avoid the driving wire stretching, causing the manipulator to wobble unsteadily. As mentioned in the previous experiment, I can replace the kite string with steel wire or reduce the weight of the manipulator to solve this problem. Second, the servo I used may have insufficient torque. When two control units move at the same time, if the proximal control unit moves in the +x direction, and the distal control unit will move in the -x direction at the same time, which will cause proximal control unit to bear a greater load. At this time, the servo controlling the proximal control unit itself is in movement, and the force bearing capacity of the opposite direction is very poor. It's likely to cause the wobbling that happens in the experiment. I can try to replace the current servo with a servo which is more powerful to solve the problem of insufficient torque.

4. Conclusions

After modifications and optimizations of the design many times, I successfully designed and made a wire-driven mechanical arm with most convenient, low-costly and safe materials, which can reduce the risks of occurrence of injury accidents and can be also used for works in high-radiation and polluted environments. It can basically achieve my original goals in the following aspects:

1) The final design of the mechanical structures of my manipulator, including the universal joints and the pre-tensioning mechanics are innovative and practical. I used the most low-cost and convenient materials and components to make a 1.35m long arm with each control unit realizing a rotation of 4 degrees of freedom (depending on the input angle). The current length of the manipulator is 1.35m, but if I can use a motor with larger torque, it is easy to increase the control unit and make it longer for industrial use.

2) The control algorithm that initially triggered me to make this manipulator was well applied in the control program, and my core algorithm was verified through experiments. In my final design, I modified the position of the wires in order to provide as large force arms as possible, which actually resulted in a major change in the algorithm. Since the initial mathematical model is correct, the algorithm modification and debugging of the program were very smooth. It can finally perform basic actions and perform both

ISSN 2706-655X Vol.5, Issue 10: 77-86, DOI: 10.25236/IJFET.2023.051012

digital and manual control, which is very flexible due to its light weight.

3) Through the study of the related works and the making of this manipulator, especially the process of identifying and resolving problems in the iterations, I have gained a deeper and more comprehensive understanding of the manipulator. I will continue to do research and explore more methods to improve the prototype. My preliminary plan on the future improvement can focus on the following areas.

a) Enhance hardware, such as enhance CPU power to achieve multi-sessions independent control of the hyper-redundant manipulator.

b) Add the real-time calculation of space kinematics and inverse kinematics, so that the manipulator can complete complex actions with practicability, such as writing, pipe transfer, etc.

c) The current control logic is feedforward control. I would like to add detection components, such as cameras, ultrasonic probes, etc., to achieve feedback control. As such, the manipulator will have automatic obstacle avoidance ability.

d) Explore more methods to improve movement accuracy, including structural optimization and compensation algorithms.

References

[1] Malone, Bob. "George Devol: a life devoted to invention, and robots." IEEE Spectrum Magazine. https://spectrum. ieee. org/automaton/robotics/industrial-robots/george-devol-a-life-de voted-to-invention-and-robots (2011).

[2] Westkämper, Engelbert, et al. "Task-oriented programming of large redundant robot motion." Robotics and Computer-Integrated Manufacturing 14.5-6 (1998): 363-375.

[3] Buckingham, Rob, and Andrew Graham. "Nuclear snake-arm robots." Industrial Robot: An International Journal (2012).

[4] Kim, Yong-Jae, et al. "A stiffness-adjustable hyperredundant manipulator using a variable neutral-line mechanism for minimally invasive surgery." IEEE transactions on robotics 30.2 (2013): 382-395.

[5] Paljug, Eric, Timothy Ohm, and Samad Hayati. "The JPL serpentine robot: a 12-DOF system for inspection." Proceedings of 1995 IEEE International Conference on Robotics and Automation. Vol. 3. IEEE, 1995.

[6] Wolf, Alon, et al. "A mobile hyper redundant mechanism for search and rescue tasks." Proceedings 2003 IEEE/RSJ International Conference on Intelligent Robots and Systems (IROS 2003)(Cat. No. 03CH37453). Vol. 3. IEEE, 2003.

[7] Brown, H. Ben, et al. "Design and control of a second-generation hyper-redundant mechanism." 2007 IEEE/RSJ international conference on intelligent robots and systems. IEEE, 2007.

[8] Hirose, Shigeo, and Shugen Ma. "Coupled tendon-driven multijoint manipulator." Proceedings. 1991 IEEE International Conference on Robotics and Automation. IEEE Computer Society, 1991.

[9] Endo, Gen, Atsushi Horigome, and Atsushi Takata. "Super dragon: A 10-m-long-coupled tendon-driven articulated manipulator." IEEE Robotics and Automation Letters 4.2 (2019): 934-941.

[10] Tang, Lei, et al. "Design of a cable-driven hyper-redundant robot with experimental validation." International Journal of Advanced Robotic Systems 14.5 (2017): 1729881417734458.

[11] Yang, Jingzhou, Potratz Jason, and Karim Abdel-Malek. "A hyper-redundant continuous robot." Proceedings 2006 IEEE International Conference on Robotics and Automation, 2006. ICRA 2006.. IEEE, 2006.

[12] McMahan, William, et al. "Field trials and testing of the OctArm continuum manipulator." Proceedings 2006 IEEE International Conference on Robotics and Automation, 2006. ICRA 2006.. IEEE, 2006.

[13] Dong, Xin, et al. "Design and analysis of a family of snake arm robots connected by compliant joints." Mechanism and Machine Theory 77 (2014): 73-91.

[14] Liu, Shuntao, et al. "Development of a dexterous continuum manipulator for exploration and inspection in confined spaces." Industrial Robot: An International Journal (2016).

[15] Wooten, Michael B., and Ian D. Walker. "A novel vine-like robot for in-orbit inspection." 45th International Conference on Environmental Systems, 2015.

[16] Xu, Wenfu, Tianliang Liu, and Yangmin Li. "Kinematics, dynamics, and control of a cable-driven hyper-redundant manipulator." IEEE/ASME Transactions on Mechatronics 23.4 (2018): 1693-1704.

[17] Huang, Long, et al. "Design and Validation of a Novel Cable-Driven Hyper-Redundant Robot Based on Decoupled Joints." Journal of Robotics 2021 (2021).